0026-895X/00/040679-08$3.00/0

MOLECULAR PHARMACOLOGY, **57:**679–686 (2000).

New Advances in the Transport of Doxorubicin through the Blood-Brain Barrier by a Peptide Vector-Mediated Strategy

CHRISTOPHE ROUSSELLE, PHILIPPE CLAIR, JEANNE-MARIE LEFAUCONNIER, MICHEL KACZOREK, JEAN-MICHEL SCHERRMANN, and JAMAL TEMSAMANI

Institut National de la Santé et de la Recherche Médicale U26, Hôpital Fernand Widal, Paris, France (C.R., J.-M.L., J.-M.S.); and Synt:em, Nîmes, France (P.C., M.K., J.T.)

Received June 30, 1999; accepted January 4, 2000

This paper is available online at http://www.molpharm.org

ABSTRACT

Many therapeutic drugs are excluded from entering the brain, due to their lack of transport through the blood-brain barrier (BBB). To overcome this problem, we have developed a novel method in which short, naturally derived peptides (16–18 amino acids) cross the cellular membranes of the BBB with high efficiency and without compromising its integrity. The antineoplastic agent doxorubicin (dox) was coupled covalently to two peptides, D-penetratin and SynB1. The ability of dox to cross the BBB was studied using an in situ rat brain perfusion technique and also by i.v. injection in mice. In the brain perfusion studies, we first confirmed the very low brain uptake of free radiolabeled dox because of the efflux activity of P-glycoprotein at the BBB. By contrast, we have demonstrated that when dox is coupled to either the D-penetratin or SynB1 vectors, its uptake was increased by a factor of 6, suggesting that the vectorized dox bypasses P-glycoprotein. Moreover, using a capillary depletion method, we have shown that vectorization of dox led to a 20-fold increase in the amount of dox transported into brain parenchyma. Intravenous administration of vectorized dox at a dose of 2.5 mg/kg in mice led to a significant increase in brain dox concentrations during the first 30 min of postadministration, compared with free dox. Additionally, vectorization led to a significant decrease of dox concentrations in the heart. In summary, our results establish that the two peptide vectors used in this study enhance the delivery of dox across the BBB.

Drug delivery into the brain is often restricted by the blood-brain barrier (BBB), which regulates the exchange of substances between the peripheral circulation and the central nervous system. BBB acts first as an anatomical barrier because of the monolayer of endothelial cells, which are its main component. They exhibit specific properties such as the intercellular tight junctions, which prevent paracellular transport. More recently, the 170-kDa ATP-dependent efflux pump P-glycoprotein (P-gp), first described as participating in the multidrug resistance (MDR) mechanisms of tumor-cell drug resistance (Juliano and Ling, 1976) has been shown to be present at the luminal site of the endothelial cells of the BBB (Cordon-Cardo et al., 1989). As a result of the P-gp functional orientation (i.e., from brain to blood), P-gp may restrict the brain entrance or increase the brain clearance of a broad number of therapeutic compounds, including cytotoxic drugs (Gottesman and Pastan, 1993; Tsuji, 1998). As a consequence of P-gp expression at the BBB interface and overexpression at the tumoral cell level, the bioavailability of anticancer agents, which may act within the cellular compartment to treat brain tumors, is extremely low, which explains the failure of brain tumor chemotherapy (Blasberg and Groothuis, 1986). To overcome the limited access of drugs to the brain, different methods have been developed that achieve BBB uptake. Most of these methods are invasive and are characterized by intraventricular drug infusion or disruption of the BBB (Chamberlain et al., 1993; Kroll and Neuwelt, 1998). In the case of chemotherapeutic agents, few studies have explored the structural modification of drugs to bypass MDR (Klopman et al., 1997) or coadministration of the drug with P-gp modulators that inhibit the effect of P-gp at the BBB (Colombo et al., 1994; Drion et al., 1996; Hughes et al., 1998). Carrier-based approaches have also been developed. They consist, for example, of increasing drug delivery to the brain by the use of liposomes and nanoparticles (Huwyler et al., 1996; Mayer, 1998; Schroeder et al., 1998) or attachment of the drug to peptide-vectors transported into the brain by absorptive transcytosis through the BBB (see Pardridge, 1997, and references therein).

The pegelin and penetratin peptides (18 and 16 amino acids, respectively) translocate efficiently through biological membranes and have provided the basis for the development

This study was supported partly by the Anvar Languedoc Roussillon and by the European Economic Community (contract no. BIO-CT98–0227).

This article is dedicated to Prof. Alain Bonnet, who passed away in November 1999.

ABBREVIATIONS: BBB, blood-brain barrier; P-gp, P-glycoprotein; dox, doxorubicin; MDR, multidrug resistance; TFA, trifluoroacetic acid; DMF, dimethylformamide; TDA, tissue distribution advantage.

of new peptide-conjugated drugs for transport through BBB. Pegelin (such as SynB1) peptides are derived from natural peptides called protegrins (Harwig et al., 1995; Mangoni et al., 1996). They possess an amphipathic structure in which the positively charged and hydrophobic residues are separated in the sequence. They are thought to form an antiparallel β-sheet, constrained by two disulfide bridges (Aumelas et al., 1996). Replacement of the four cysteines with serines leads to linear peptides (pegelin) that are able to cross cell membranes efficiently without any cytolytic effect. The penetratin peptides are derived from the transcription factor antennapedia (Derossi et al., 1998). The region of the homeodomain of antennapedia responsible for internalization has been mapped to its third helix (Derossi et al., 1994). This finding has led to the demonstration that a 16-amino-acid peptide corresponding to the third helix translocates efficiently across biological membranes.

The aim of this study was to assess the efficacy of these peptides as vectors for delivery of drugs through the BBB. Doxorubicin (dox) was chosen as the vectorized drug because it is a widely used antineoplastic agent in the treatment of several cancers and has been shown to poorly cross the BBB and not to penetrate the brain tumor cells because of MDR mechanisms (Ohnishi et al., 1995; Mankhetkorn et al., 1996). Various methods, such as the in situ brain perfusion technique (Takasato et al., 1984), have been used to evaluate brain uptake kinetics of drugs. We have applied this latter technique with some modifications (Smith, 1996). This method is simple and sensitive and allows the BBB to be exposed for a short time (15 to 90 s) to a drug under infusion conditions where the fluid composition and the rate of infusion are controlled. Complementary techniques were associated with it to measure the fraction of dox trapped into microvessel cells or present in brain parenchyma (Triguero et al., 1990). Finally, we investigated the overall bioavailability of the free and peptide-conjugated dox in mice. The results obtained in this study indicate that this approach could be used as a safe and effective delivery system for the transport of drugs across the BBB.

Materials and Methods

Animals and Reagents

Male Sprague-Dawley rats (250–350 g; 8 weeks) were obtained from Iffa-Credo (L'Arbresle, France). Mice NMRI-nude (29 g; 7 weeks) were obtained from Janvier Breeding Center (Le Genest Saint Isle, France). Animals were maintained under standard conditions with ad libitum access to food and water. Rats were anesthetized with an i.p. injection of the combination ketamine hydrochloride (50 mg/ml; 70 mg/kg; Parke-Davis, Courbevoie, France) and diazepam (5 mg/ml; 7 mg/kg; Roche; Neuilly-Sur-Seine, France). Mice were anesthetized with isoflurane before sacrifice. The ethical rules of the French Ministry of Agriculture for experimentation with laboratory animals (law no. 87–848) were followed.

Preparation and Characterization of Peptide Conjugates

Peptide Synthesis. The peptides were assembled by conventional solid phase chemistry using a 9-fluorenylmethoxycarbonyl/tertiobutyl protection scheme (Atherton and Sheppard, 1989) and purified on preparative C18 reversed phase HPLC after trifluoroacetic acid (TFA) cleavage/deprotection. The lyophilized products were assessed by C18 reversed phase analytic HPLC. The peptide sequences were SynB1 (RGGRLSYSRRRFSTSTGR; molecular mass, 2099 D) and D-penetratin (rqikiwfqnrrmkwkk, the amino acids are in D form; molecular mass, 2245 D).

Dox-D-Penetratin Synthesis. Dox hydrochloride (1 molar equivalent; Fluka, Buchs, Switzerland) was suspended in dimethylformamide (DMF) containing diisopropylamine (2 molar equivalents; Fluka) (Fig. 1). *N*-hydroxysuccinimidylmaleimidopropionate (1 molar equivalent; Fluka) was added and incubated for 20 min. The thiol-containing peptide (either as a cysteine or as amino-terminal 3-mercaptopropionic acid solubilized in DMF) was then added to this reaction mixture, followed by a 20-min incubation. The acceptance criteria for the peptide and conjugates was HPLC purity of >98% at 215 and 480 nm in accordance with the molecular weight and fragmentation pattern for mass spectrometry. The molecular mass was found to be 3005 Da.

Dox-SynB1 Synthesis. Dox hydrochloride was suspended in DMF containing diisopropylamine (Fig. 1). Succinic anhydride (1 molar equivalent; Fluka) dissolved in DMF was added and incubated for 20 min. The resulting dox hemisuccinate was then activated by addition of benzotriazol-1-yl-oxopyrrolidinephosphonium hexafluorophosphate (1.1 molar equivalents; Novabiochem) dissolved in DMF. The peptide was then added to the reaction mixture after 5 min of activation and left for another 20 min for coupling. Further processing and purity check of the conjugate was performed as described above. The molecular mass was 2723 Da.

Radiolabeling of Dox-D-Penetratin and Dox-SynB1. Preparations were performed as described above, except that [^{14}C]dox (55 mCi/mmol, 2.04 TBq/mol; Amersham, Les Ulis, France) was kept limiting by raising the stoichiometry of peptide, linkers, and activators to 1.3 eq in the coupling reactions. The specific activity of both compounds was (55 mCi/mmol, 2.04 Tbq/mol) and the molar ratio of dox/peptide was 1:1. The radiochemical purity was estimated to be >98% according to the 480-nm chromatograms.

Distribution Coefficient Determinations. The lipophilicity of the radiolabeled free and vectorized dox was estimated by measuring their partitioning between the perfusion buffer, pH 7.4, and 1-octanol. Distribution coefficients ($D_{octanol/buffer}$) were determined at volume ratios of 1:1 by vigorously shaking the two phases together. The samples were then incubated at 37°C for 30 min to facilitate phase separation. One sample of each phase was weighed and the radioac-

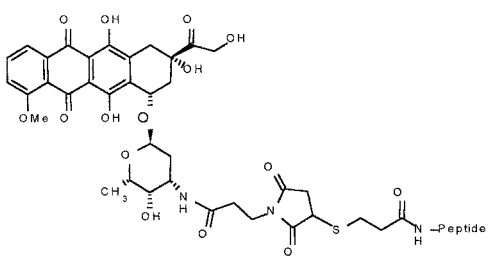

doxo-D-Penetratin

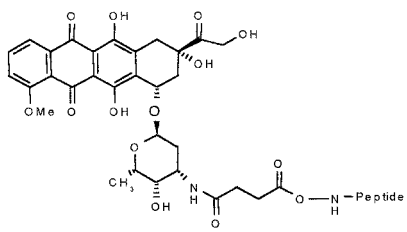

doxo-SynB1

Fig. 1. Structure of dox-D-penetratin and dox-SynB1.

tivity counted in a gamma counter. $D_{octanol/buffer}$ was calculated as: ([dpm/ml] in the octanol phase)/([dpm/ml] in the buffered saline phase). Experiments were done in triplicate and the mean of the log $D_{octanol/buffer}$ for dox, dox-D-penetratin, and dox-SynB1 were: 0.45 ± 0.06; −0.9 ± 0.08; and −1.44 ± 0.04, respectively.

Plasma Protein Binding Determination. Binding to rat plasma proteins of the radiolabeled free and vectorized dox was determined after incubation of each compound in rat plasma (Iffa Credo, L'arbresle, France) for 10 min at 37°C and ultrafiltration of the samples using the Centrifree Micropartition System (Amicon, Beverly, MA). Final concentrations in both phases were determined by counting the radioactivity as described above, and the bound fraction was calculated after three experiments. For dox, dox-D-penetratin, and dox-SynB1, mean values of bound fractions were: 87.66 ± 1.76, 99.49 ± 0.02, and 95.8 ± 0.38%, respectively.

In Situ Brain Perfusion

Blood to Brain Transfer of Dox. We used the in situ brain perfusion technique of Takasato et al. (1984) as described previously (Rousselle et al., 1998). The perfusion fluid was a bicarbonate-buffered physiological saline (128 mM NaCl, 24 mM $NaHCO_3$, 4.2 mM KCl, 2.4 mM NaH_2PO_4, 1.5 mM $CaCl_2$, 0.22 mM $MgSO_4$, and 9 mM D-glucose, pH 7.4) infused at a flow rate of 10 ml/min. For some experiments, rat brains were perfused with plasma obtained the same day from heparinized donor rats at a flow rate of 5 ml/min, which is sufficient to perfuse the ipsilateral hemisphere at a reasonable pressure. [^{14}C]Dox (0.3 μCi/ml), [^{14}C]dox-D-penetratin (0.1 μCi/ml), and [^{14}C]dox-SynB1 (0.1 μCi/ml) were infused into the internal carotid artery for 60 s. [^{3}H]Sucrose (12.3 Ci/mmol; 1 μCi/ml; NEN, Paris, France) was used for each experiment as a marker of the BBB integrity. Some rats (n = 9) were also pretreated 5 min before perfusion with i.v. (±)-verapamil hydrochloride (1 mg/kg; Sigma, St. Quentin Fallavier, France) dissolved in 0.5 ml of 0.9% NaCl.

At the end of the perfusion, the rat was decapitated and the brain quickly removed. The right cerebral hemisphere was dissected on ice in six brain areas (frontal, occipital and parietal cortex, thalamus, hippocampus, and striatum). Brain regions and 50 μl of perfusion fluid were placed in preweighed scintillation vials and weighed. Brain and perfusion fluid samples were digested for 2 h in 1 ml of Soluene-350 (Packard, Rungis, France) at 60°C. Scintillation cocktail (10 ml; Picofluor, Packard) was added to each vial and the tracer contents were assessed by dual-label liquid scintillation counting program in a Tri-Carb model 1900TR liquid scintillation counter (Packard).

Dox uptake was expressed as a single-time-point, unidirectional transfer constant (K_{in}). Briefly, calculations were accomplished as described (Smith, 1996) from the relationship $K_{in} = (Qtot - Vv \cdot Cpf) / T \cdot Cpf)$, where Qtot is the measured quantity of [^{14}C]dox in brain (vascular and extravascular) at the end of the experiment, Vv is the cerebral vascular volume, Cpf is the perfusion fluid concentration of [^{14}C]dox, and T is the perfusion time in seconds. Vv was evaluated by the sucrose space and calculated by the ratio between radioactivity of [^{3}H]sucrose (expressed in dpm of sucrose per gram of brain) and the perfusate sucrose concentration.

Washing Procedure. For this set of experiments, we used a dual-syringe infusion pump (Harvard Apparatus, Les Ulis, France) with one syringe containing the bicarbonate-buffered physiological saline with the radiotracer (syringe A) and the other without radiotracer (syringe B). The carotid catheter was connected to a four-way valve (Hamilton, Bonnaduz, Switzerland). After the carotid cannulation was completed and the appropriate connections were made, syringe A was discharged at a rate of 10 ml/min for 60 s. Syringe A was switched off and syringe B was switched on simultaneously to initiate the wash-out of the capillary space. After 30 s, the rat was decapitated. The transfer constant was measured using the equation K_{in} = Qtot / T · Cpf, where Qtot is the quantity of [^{14}C]dox in the extravascular brain.

Distribution in Brain Compartments. The distribution of [^{14}C]dox between brain microvascular and parenchymal compartments was assessed using the capillary depletion method of Triguero et al. (1990) with some modifications (Benrabh and Lefauconnier, 1996). Rats were perfused as described for the washing procedure. At the end of the wash-out, the right cerebral hemisphere was removed, cleaned of meninges and choroid plexus, weighed, and homogenized in 3.5 ml of capillary buffer (10 mM HEPES, 141 mM NaCl, 4 mM KCl, 1 mM NaH_2PO_4, 2.8 mM $CaCl_2$, 1 mM $MgSO_4$, and 10 mM D-glucose, pH 7.4) on ice. After 15 strokes, 4 ml of a chilled 40% neutral dextran solution was added to obtain a final concentration of 20%. All homogenizations were performed at 4°C in a very short time. After taking an aliquot of homogenate, the solution was centrifuged at 5400*g* for 15 min at 4°C in a swinging-bucket rotor. The pellet and supernatant were carefully separated and counted in the liquid scintillation counter. The pellet was composed mainly of brain capillaries and the supernatant reflected brain parenchyma.

Dox distribution in brain compartments was expressed as distribution volume (Vd; μl/g), defined as Vd = Qtis / Cpf, where Qtis is the measured quantity of [^{14}C]dox in brain compartments (total dpm per compartment/brain tissue weight) and Cpf is the perfusion fluid concentration (dpm/milliliters of perfusate).

Statistical Analysis. All experiments were performed on three to six rats. Data are expressed for individual cerebral areas or as the main value of the right cerebral hemisphere. Statistical comparisons conducted herein were accomplished by Student's test or ANOVA. Bonferroni's multiple comparison test was used post hoc only when ANOVA results were significant. Statistical difference was accepted at the $P < .05$ significance level. Data are presented as mean ± S.E.

Intravenous Administration in Mice

Dox and dox-SynB1 were i.v. injected in female Nude mice (via the tail vein) at a dose of 2.5 mg/kg (mg base of dox/kg; in 200 μl of NaCl 0.9%), which corresponded to 0.5 μCi per animal. At 1, 5, 15, 30, 60, 180, 480, and 1280 min after injection, animals (five animals per group) were anesthetized before sacrifice. Mice were sacrificed by cardiac puncture and blood samples were collected in glass tubes containing EDTA anticoagulant. Brain, heart, lungs, liver, and kidneys were removed for determination of total radioactivity. The plasma was recovered after centrifugation. The tissue samples were collected in scintillation tubes, immersed in liquid nitrogen, and stored at −20°C until analysis. The samples were fully used to quantify the radioactivity, and the radioactivity data was corrected in accordance with the quenching calculation. After radioactivity measurement, the results were transformed in micrograms of dox-equivalent per gram of plasma or tissue and represented as a mean ± S.E. of four to five animals.

Tissue to plasma partition coefficient (K_p) was determined by dividing the area under the average curve (AUC) calculated by the linear trapezoidal method for each time point between the tested tissue and plasma as $K_{p\ tn\rightarrow tn+1}$ = $AUC_{\ tn\rightarrow tn+1}$ tissue / $AUC_{\ tn\rightarrow tn+1}$ plasma.

The term "tissue distribution advantage" (TDA) previously used by others (Malhotra et al., 1994) was introduced to evaluate the relative uptake behavior of dox-SynB1 versus free dox. TDA was calculated as the ratio of the respective tissue to plasma partition coefficients of the conjugated dox versus free dox at each time point according to $TDA = K_{p\ tn\rightarrow tn+1\ dox\text{-}SynB1} / K_{p\ tn\rightarrow tn+1\ dox}$. A TDA > 1 will define a specific tissue targeting of SynB1.

Stability In Vitro and In Vivo

Dox-SynB1 (1 ml) solution (2 mg/ml) was mixed with 4 ml of rat or mouse plasma (obtained from Iffa-Credo). At various times (0, 15, 25, 30, 40, 45, 60, 120, 180, and 210 min), 250-μl aliquots were withdrawn and quenched in 1 ml of acid mixture (H_2O/TFA 0.1%). The vectorized dox and metabolites were then extracted from plasma by applying the sample on a C18 solid phase extraction cartridge and

eluting in 500 μl of acetonitrile/isopropanol/H_2O/TFA (50/20/30/5 ml) solution. The samples were then analyzed by HPLC on C18 column using acetonitrile/water gradient. The percentage of nondegraded vectorized dox and released dox was calculated.

In the in vivo stability study, mice were i.v. injected with dox-SynB1 at a dose of 2.5 mg/kg (milligram base of dox). The percentage of free released dox was measured by HPLC.

Results

First, the tolerance of the BBB for the compounds used in this study was explored. [^{3}H]sucrose was used as a marker of brain vascular volume because it does not measurably penetrate the BBB during brief periods of perfusion. When 0.05 mg of either free or coupled dox were perfused, the vascular volumes were not significantly different among brain regions in all groups. They were about 10 μl/g of brain and of the same order of magnitude as those found in previous reports using the in situ brain perfusion method (Drion et al., 1996; Rousselle et al., 1998). This indicates that the permeability of the BBB was not changed. However, when 0.8 mg of dox-D-penetratin was perfused in rats, brain vascular volumes were 2-fold larger than those observed with other compounds or with 0.05 mg of dox-D-penetratin. Interestingly, the use of D-penetratin alone at the same concentration did not change the BBB permeability (data not shown), suggesting that alteration of the BBB may be caused by the complex dox-D-penetratin. We therefore used 0.05 mg of dox-D-penetratin or dox-SynB1 for the following brain perfusion experiments.

We then compared the brain uptake of free and coupled radiolabeled dox by measuring the total radioactivity in the brain after 60 s of brain perfusion. This perfusion time was chosen because it is short enough to limit the risks of drug metabolism or efflux from brain to blood but high enough to measure reasonable quantities of radiolabeled dox in brain tissues compared with the background noise of the detection method. Figure 2 shows that conjugation of dox with peptide vectors significantly enhances its brain uptake. An average of 6-fold increase in brain uptake was obtained for both dox-D-penetratin and dox-SynB1. To assess the brain distribution of these compounds, the brain was dissected into various areas: frontal, parietal, and occipital cortex, thalamus, hippocampus, and striatum. In rats perfused with dox, the brain uptake of this compound was very low and ranged from 0.18 ± 0.04 μl/s/g for the striatum to 0.78 ± 0.22 μl/s/g for the occipital cortex. Vectorization with either D-penetratin or SynB1 significantly increased the brain uptake of dox after 60 s of buffer perfusion in all six gray areas. The brain uptake of dox-SynB1 ranged from 1.6 ± 0.2 μl/s/g for the frontal cortex to 2.7 ± 0.4 μl/s/g for the parietal cortex. In the case of dox-D-penetratin, the brain uptake ranged from 1.4 ± 0.3 μl/s/g for the striatum to 3.6 ± 0.3 μl/s/g for the parietal cortex.

To evaluate whether free or coupled dox has actually crossed the BBB or is simply trapped within brain endothelial cells, two experiments were performed. In the first one, the brain was perfused for 60 s with radiolabeled compounds in physiological saline followed by a 30-s washing with tracer-free saline to remove tracer bound to the capillary luminal membrane. The total radioactivity measured was then compared with the one in animals that did not receive the wash-out procedure. After the washing procedure, the cerebral uptake of free and vectorized dox was significantly reduced, indicating that this procedure removed any [^{14}C]dox trapped within the microvessels or bound to the luminal membrane of its endothelium (Fig. 3). However, in rats perfused with either dox-D-penetratin or dox-SynB1, the brain uptake was still significantly increased (2.14 ± 0.23 and 1.50 ± 0.28 μl/s/g, respectively) compared with that of dox alone (0.25 ± 0.09 μl/s/g). In the second experiment, distribution in the brain capillary and parenchymal compartment was measured after perfusion and wash-out using the capillary depletion method of Triguero et al. (1990), which separates the whole brain into endothelial enriched (pellet) and depleted (supernatant) fractions. This procedure distinguishes between compounds remaining in the endothelial cells from those having crossed the abluminal endothelial membrane to enter the brain parenchyma. By this method, we have observed that about 50% of the dox-derived radioactivity was associated with the capillary, whereas less than 30% of the vectorized dox-derived radioactivity was in the endothelial

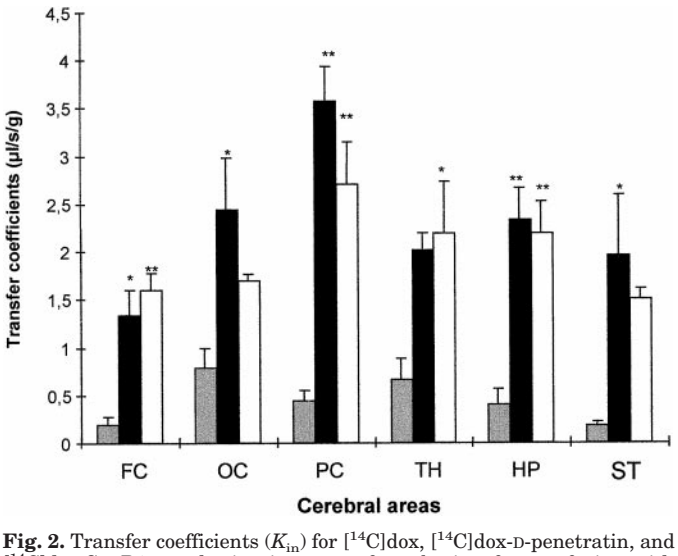

Fig. 2. Transfer coefficients (K_{in}) for [^{14}C]dox, [^{14}C]dox-D-penetratin, and [^{14}C]dox-SynB1 uptake in six areas of rat brain after perfusion with buffer. Each bar represents a mean (± S.E.) for $n = 4$ animals. The animals were perfused for 60 s with 5.4 nmol/ml of dox (gray columns), 1.8 nmol/ml of dox-D-penetratin (filled columns), and 1.8 nmol/ml of dox-SynB1 (open columns). FC, OC, and PC, frontal, occipital and parietal cortex; TH, thalamus, HP, hippocampus; ST, striatum. $^{**}P < .01$; $^{*}P < .05$ versus free dox.

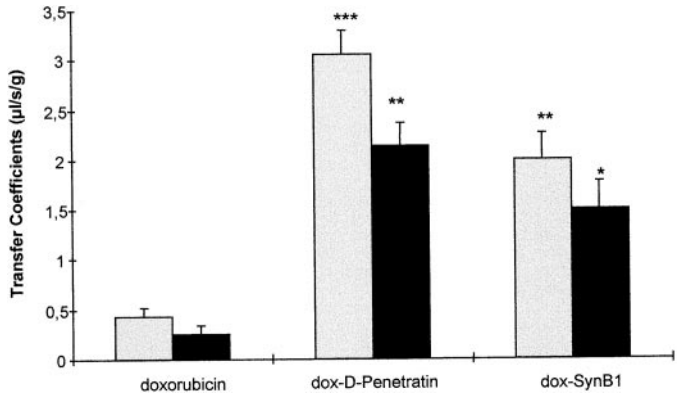

Fig. 3. Transfer coefficients (K_{in}) for [^{14}C]dox, [^{14}C]dox-D-penetratin, and [^{14}C]dox-SynB1 uptake in right hemisphere of rat brain after 60-s perfusion with buffer and 30 s of wash-out. Values are mean ± S.E. ($n = 4$ rats). $^{***}P < .001$; $^{**}P < .01$; $^{*}P < .05$ versus free dox. Filled columns, wash-out; gray columns, no wash-out.

cells after 60 s of perfusion followed by 30 s of wash-out (Fig. 4). In the parenchymal compartment, the ratio of vectorized dox versus free dox was about 20 for both peptide-vectors.

To compare the vectorization of dox with the effect of a P-gp inhibitor, dox uptake was evaluated in rats pretreated with (±)-verapamil. This calcium-channel blocker is a P-gp inhibitor commonly used to reverse MDR in cell culture (Ford and Hait, 1990). Pretreatment with verapamil only slightly increased the cerebral uptake of dox after 60 s of perfusion and 30 s of wash-out (Table 1). However, this increase was not significant. Moreover, no change in brain uptake of vectorized dox was observed after pretreatment with verapamil.

Finally, we investigated the effect of plasma protein binding on brain transfer of free and vectorized dox (Fig. 5). When the perfusion buffer was replaced by rat plasma, a dramatic decrease in dox-D-penetratin cerebral uptake was observed (0.05 versus 2.30 μl/s/g). The brain uptake of free dox was also significantly reduced (0.07 versus 0.44 μl/s/g) as it was for dox-SynB1 (0.60 versus 2.20 μl/s/g). Similar results were obtained after perfusion in the presence of 5% BSA in the saline buffer (data not shown). This is not surprising, because it has been shown previously that dox binds to plasma proteins and principally to albumin (Celio et al., 1982). Cerebral transfer coefficients of vectorized dox in plasma are also well correlated with the plasma protein binding measured in our study by ultrafiltration (87.8% for dox, 99.5% for dox-D-penetratin, and 95.8% for dox-SynB1). Consequently, we considered the possibility that the high protein binding of our peptide vectors may compromise dox delivery to the brain after peripheral administration.

To check this last hypothesis and to confirm the ability to distribute more dox in the brain, we carried out in vivo experiments using i.v. injection. Free and SynB1-conjugated radiolabeled dox were injected into mice at a dose of 2.5 mg/kg (mg base of dox) via the tail vein. After different time points, the mice were sacrificed and the total radioactivity in plasma, brain, heart, lungs, kidneys, and liver was counted. After i.v. injection, the tissue and plasma distribution of dox-derived radioactivity were dramatically modified when the drug was conjugated to SynB1 (Fig. 6A). The plasma concentrations were higher for dox-SynB1 and decreased less rapidly than for the free dox. The brain distribution of dox was also apparently improved when the drug was conjugated to SynB1 (Fig. 6B). Interestingly, in the heart, where dox exerts its major toxicity, vectorization significantly reduced the dox concentrations (Fig. 6C). A similar decrease in accumulation of vectorized dox was observed in lungs. In kidneys and liver, a slight decrease in total radioactivity was observed for dox-SynB1 1 h after administration (data not shown). We also carried out a small-scale pilot experiment using D-penetratin as a vector and similar results as for SynB1 were obtained (data not shown).

To assess whether the modifications in tissue distribution observed with dox-SynB1 versus free dox were caused only by an alteration of dox-SynB1 plasma pharmacokinetics, we calculated tissue-to-plasma-partition coefficients at each time point (Table 2) and compared them with those of dox alone. The calculated TDA was found to be >1 in brain during the first 30 min after administration, showing a more important brain uptake of dox-SynB1 than would have been expected from the observed increase of dox-SynB1 plasma levels (Fig. 7). In contrast, TDAs were <1 for heart, lungs, liver, and kidneys, showing a reduction in tissue exposure for these organs at all time points.

To assess the stability and the fate of the dox-vector complex, we have carried out two preliminary experiments. In the first experiment, dox-SynB1 was incubated in rat and mouse plasma in vitro, and after various times, the fate and stability of the dox-SynB1 was analyzed by HPLC. Our results show that the conjugate has a degradation half-life of about 15 min in mice and rat plasma. The percentage of dox

TABLE 1

Transfer coefficients for [^{14}C]dox, [^{14}C]dox-D-penetratin, and [^{14}C]dox-SynB1 uptake into rat brain. Data are presented as mean ± S.E.; n = 3–6. Perfusion time was 60 s and wash-out time was 30 s. Pretreatment with verapamil was carried out 5 min before perfusion at 1 mg/kg.

	K_{in}	
	Control	Verapamil Pretreated
	$\mu l/s/g$	
Dox	0.25 ± 0.09	0.36 ± 0.01
Dox-D-Penetratin	2.31 ± 0.46	2.15 ± 0.34
Dox-SynB1	1.20 ± 0.17	1.31 ± 0.13

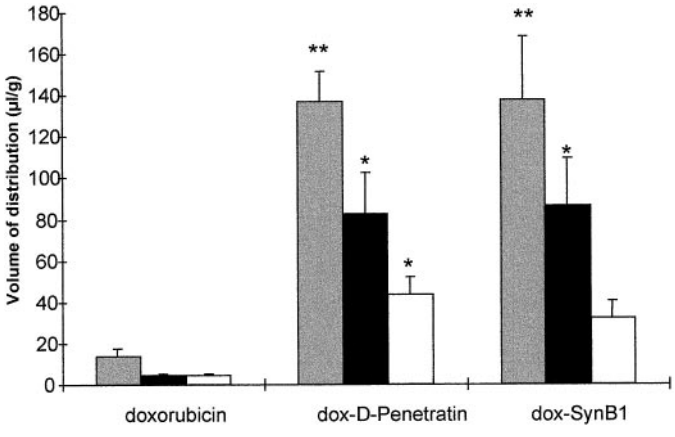

Fig. 4. Distribution volumes of [^{14}C]dox, [^{14}C]dox-D-penetratin, and [^{14}C]dox-SynB1 in vascular pellet and supernatant fractions after wash-out after the capillary depletion method. Values are mean ± S.E. (n = 4 rats). **P < .01; *P < .05 versus free dox. Gray columns, homogenate; filled columns, parenchyma; open columns, endothelial cells.

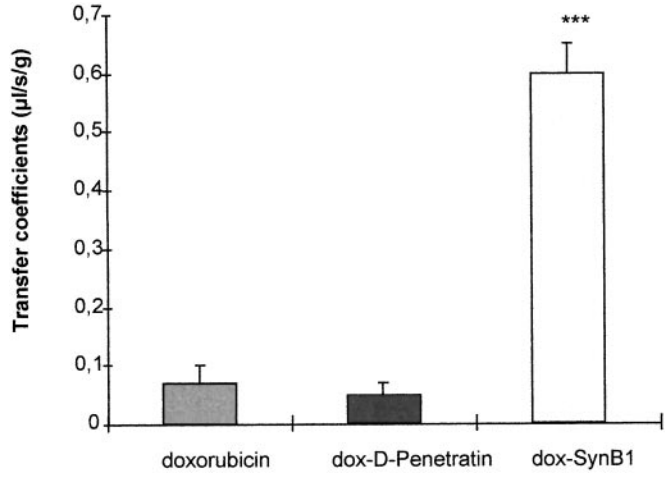

Fig. 5. Transfer coefficients (K_{in}) for [^{14}C]dox, [^{14}C]dox-D-penetratin, and [^{14}C]dox-SynB1 uptake in rat brain after perfusion with plasma. Each bar represents a mean ± S.E. (n = 4 rats). Perfusion time was 60 s. ***P < .001 versus free dox.

released was about 8% at 15 min. The rest of products corresponded mainly to degradation in the peptide. In the second experiment, dox-SynB1 was injected into mice and the percentage of released dox was measured by HPLC. In plasma, we found that about 3% of free dox was released from dox-SynB1 after 5 min postadministration (data not shown).

Discussion

The discovery that synthetic peptides derived from natural peptides can be used successfully to deliver biologically active substances inside live cells (Derossi et al., 1998; Schwarze et al., 1999) has provided the basis for developing new effective strategies for drug delivery into the brain. For this reason we have coupled the anticancer drug dox to two different peptides: D-penetratin and SynB1, which were expected to increase the delivery of dox to rat brain.

We first evaluated the brain uptake of free and coupled dox after 60 s of in situ rat brain perfusion. Under these conditions, we only observed a low uptake of dox, comparable with values reported previously by Ohnishi et al. (1995) using the same method. However, this permeability is lower than would be expected based on the lipophilicity of the compound (log $D_{octanol/buffer}$ = 0.45). This low brain permeability could be explained by the efflux activity of P-gp at the BBB. Dox is actually transported by P-gp expressed at the brain capillaries in the physiological state (Ohnishi et al., 1995; Van Asperen et al., 1999) and could also be transported by the more recently characterized MDR-associated protein mrp1 (Abe et al., 1994). To overcome MDR mechanisms, dox was given in combination with P-gp inhibitor. However, if such drug combinations are effective in vitro, the high concentration of P-gp inhibitors necessary to overcome drug efflux limits their clinical application. Furthermore, coadministration of anticancer drugs and P-gp modulators may alter anticancer drug pharmacokinetics, leading to an exacerbation of anticancer drug toxicity (Krishna et al., 1997).

By coupling dox to D-penetratin and SynB1, we expected to increase its uptake in the brain and circumvent the efflux activity of P-gp. It is noteworthy that the coupling makes the dox less lipophilic (log$D_{octanol/buffer}$ = 0.45 for dox, −0.9 for dox-D-penetratin, and −1.44 for dox-SynB1), which in fact should reduce the permeability through the BBB. However, a significant increase in dox-derived radioactive brain uptake was obtained for the conjugated drug compared with free dox for all six gray areas studied. This increase in brain uptake obtained for both vectors might be explained by the translocation properties of these vectors and also by the fact that vectorized dox is not recognized by the P-gp. This is confirmed by pretreatment with verapamil, which did not change the brain uptake of the coupled dox, and only a slight increase was observed for free dox. To demonstrate that vectorized dox is not trapped inside the endothelial cells but actually crosses the BBB, we carried out the wash-out procedure and the capillary depletion method. Our results indicate that the amount of vectorized dox that was delivered to the brain parenchyma was about 20-fold higher than free dox, suggesting the efficiency of these peptide-vectors in delivering dox to the brain parenchyma. However, we observed a decrease in brain uptake (especially for dox-D-penetratin) when the cerebral perfusion was performed with plasma for a short period of time (60 s). Over a longer period of time, protein binding does not seem to hamper the brain distribution of vectorized dox as shown by the results obtained after i.v. administration in mice. These results are consistent with the hypothesis that the bound drug in plasma can dissociate from proteins and thus becomes available for brain transfer. When the permeability of the brain capillaries for the free drug is sufficiently high, a new equilibrium is rapidly achieved inside the capillaries leading to the release of some bound drug into a free form that then becomes available for brain transfer (Pardridge and Landaw, 1984; Jolliet-Riant and Tillement, 1999).

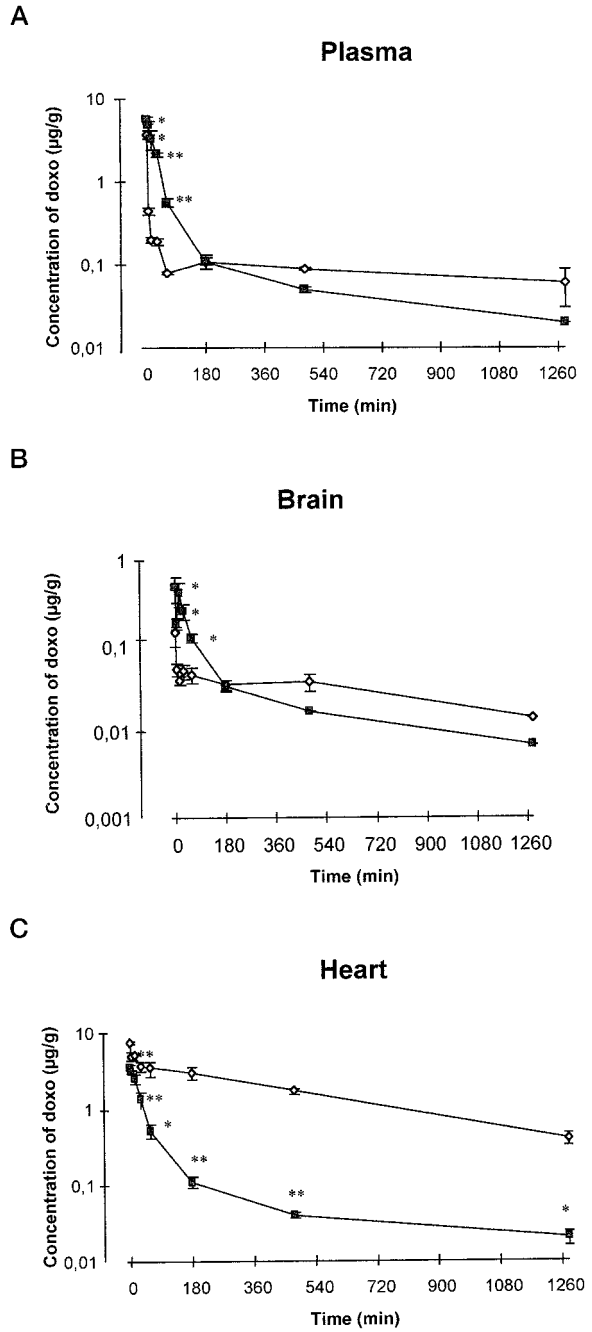

Fig. 6. Plasma and tissues distribution after i.v. administration of free dox (◇) and dox-SynB1 (■) at a dose of 2.5 mg/kg. The concentrations are represented in microgram equivalents of dox on the basis of radioactivity measurements. The bars represent the S.E. of four to five animals. A, plasma; B, brain; C, heart. *$P < .05$; **$P < .01$ versus free dox.

TABLE 2
The area under plasma and tissues concentration curve (AUC) values were calculated for both dox-SynB1 and free dox from the time of injection to the given time point. The ratio of AUC tissue/AUC plasma of free and vectorized dox is represented here.

Time (min)	AUC Tissue/AUC Plasma									
	Brain		Heart		Lungs		Liver		Kidneys	
	dox	dox-SynB1	dox	dox-SynB1	dox	dox-SynB1	dox	dox-SynB1	dox	dox-SynB1
1	0.017	0.044	0.9	0.325	1.165	0.307	0.311	0.324	4.414	1.511
5	0.037	0.06	2.286	0.578	3.039	0.594	0.974	0.586	7.675	3.291
15	0.059	0.069	5.041	0.65	6.503	0.809	3.109	0.746	17.341	4.183
30	0.086	0.09	7.787	0.674	9.33	1.002	5.981	0.934	25.264	4.585
60	0.136	0.104	11.072	0.677	12.604	1.174	8.967	1.222	34.52	4.959
180	0.233	0.132	18.723	0.734	22.365	1.463	12.34	1.875	50.365	5.45
480	0.295	0.153	20.959	0.767	29.263	1.793	13.164	2.492	53.588	5.924
1280	0.32	0.175	17.63	0.768	30.683	2.868	12.085	3.269	48.984	6.136

The pharmacokinetic profile of vectorized dox in plasma and tissues showed marked differences compared with free dox. In plasma, vectorization led to higher initial concentrations of dox-SynB1 than for free dox and the blood clearance of the vectorized dox was reduced during the first 180 min (area under the curve of dox-SynB1 was 5.51 times higher than for dox), allowing the compound to be more exposed to brain and other tissues. Assuming that dox-SynB1 is hydrolyzed in plasma with a stability half-life in plasma of about 15 min, this suggests that during at least 2 to 3 half-lives (i.e., 30 to 45 min) corresponding to the time window of the distribution phase, a higher tissue exposure was obtained for dox-synB1 than for free dox.

Surprisingly, we found different distribution patterns of vectorized dox in tissues compared with free dox, suggesting a tissue-specific uptake of dox-SynB1. In fact, certain tissues like heart, lungs, and, to a lower extent, kidneys and liver, had a lower uptake of dox-SynB1 than free dox (TDA were in general <0.4). The lower accumulation in heart could be of great clinical interest, because the use of dox in chemotherapy has been hampered by its cardiotoxicity (Lefrak et al., 1973). The lower uptake observed for vectorized dox in lungs can also be regarded as an interesting property, because the lung is usually the first exposed organ after the i.v. route and is known to markedly distribute cationic molecules, causing toxicity (Bummer et al., 1995). Brain, rather than these tissues, seemed to accumulate vectorized dox. During the first 180 min after administration, the brain levels of dox-SynB1 were higher than those of free dox. Nevertheless, this might result from the increase in the systemic bioavailability of dox-SynB1. To verify this hypothesis, we calculated the brain distribution advantage, which shows that during the first 30 min after administration, brain uptake enhancement was higher than that observed in plasma. This observation confirms that during the period in which dox-SynB1 is not too much hydrolyzed, the more pronounced brain uptake results from the dox-SynB1 chemical entity interaction with endothelial cells of the BBB. This effect observed in vivo is well supported by the data from the in situ brain perfusion method, which showed a rapid transcytosis process across the BBB. For longer time-points, degraded forms of dox-SynB1 being predominant, no enhancement in dox brain uptake was observed. This suggests that enhancing the stability of the vectors might enhance the brain uptake of dox. A time balance between the kinetics of vector degradation and drug release in the targeted tissue has to be found by using less degradable amino acid sequences and appropriate linker. The challenge now is to develop peptide-vectors stable enough in plasma and a linker that will allow the drug to be cleaved off once it has crossed the BBB.

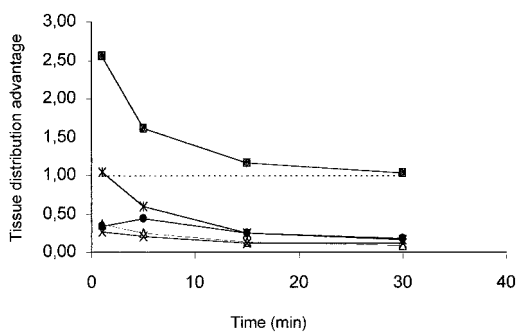

Fig. 7. TDA was calculated as the ratio of the respective tissue to plasma partition coefficients of the vectorized dox versus free dox at each time point. ----, plasma; ■, brain; △, heart; ×, lungs; ∗, liver; ●, kidneys.

In summary, the tissue distribution shows two different organ patterns: tissues with less exposure (heart, lungs, liver, and kidneys) and tissues with higher exposure (brain). This clearly shows a tissue-specific uptake of the vectorized dox.

The mechanism by which these peptides cross the BBB is still under investigation. These peptides translocate efficiently across cell membranes and, at least in the case of D-penetratin, cell internalization does not seem to involve classical receptor-mediated endocytosis (Derossi et al., 1996). It is possible that once internalized, the peptides are addressed to a secretory compartment and re-exported into the brain parenchyma. Interestingly, Prochiantz and colleagues have demonstrated that homeoproteins—from which penetratin sequences were derived—can be secreted from live cells and gain access in vivo to a secretory compartment enriched in cholesterol and glycosphingolipids (Joliot et al., 1997, 1998).

These studies only test the feasibility of enhancing dox delivery to brain using peptide-vectors and do not address the pharmacodynamics of drug action in brain. It is crucial that the coupling of dox does not result in a loss of biological activity. Our preliminary experiments in cell culture using resistant cell lines show that the coupled dox with both D-penetratin and SynB1 bypasses P-gp and increases drug potency compared with free dox (unpublished observations). The next step will be to explore the antitumor potential of vectorized dox in brain tumor models and new modified peptides.

In conclusion, this study demonstrates the successful ap-

plication of the use of these peptide vectors for brain delivery of dox. A significant enhancement of dox uptake in brain was obtained after coupling dox with these peptides. Although these investigations focus on the delivery of dox, this approach should be applicable to other therapeutic drugs.

Acknowledgments

We thank Dr. Alain Prochiantz and Professor Anthony Rees for helpful advice and criticism, and Dr. Pierre Vidal for the in vitro stability work.

References

Abe T, Hasegawa S, Taniguchi K, Yokomizo A, Kuwano T, Ono M, Mori T, Hori S, Kohno K and Kuwano M (1994) Possible involvement of multidrug-resistance-associated protein (MRP) gene expression in spontaneous drug resistance to vincristine, etoposide and adriamycin in human glioma cells. *Int J Cancer* **58:**860–864.

Atherton E and Sheppard RC (1989) *Solid Phase Peptide Synthesis: A Practical Approach*. IRL Press at Oxford University Press, Oxford, England.

Aumelas A, Mangoni M, Roumestand C, Chiche L, Despaux E, Grassy G, Calas B and Chavanieu A (1996) Synthesis and solution structure of the antimicrobial peptide protegrin- 1. *Eur J Biochem* **237:**575–583.

Benrabh H and Lefauconnier JM (1996) Blood-endothelial cell and blood-brain transport of L-proline, alpha-aminoisobutyric acid, and L-alanine. *Neurochem Res* **21:**1227–1235.

Blasberg RG and Groothuis DR (1986) Chemotherapy of brain tumors: Physiological and pharmacokinetic considerations. *Semin Oncol* **13:**70–82.

Bummer PM, Aziz S and Gillepsie MN (1995) Inhibition of pulmonary surfactant biophysical activity by cationic polyamino acids. *Pharm Res* **12:**1658–1663.

Celio LA, Digregorio GJ, Ruch E, Pace JN and Piraino AJ (1982) Doxorubicin concentrations in rat plasma, parotid saliva, and bile and protein binding in rat plasma. *Arch Int Pharmacodyn Ther* **260:**180–188.

Chamberlain MC, Khatibi S, Kim JC, Howell SB, Chatelut E and Kim S (1993) Treatment of leptomeningeal metastasis with intraventricular administration of depot cytarabine (DTC 101). A phase I study. *Arch Neurol* **50:**261–264.

Colombo T, Zucchetti M and D'Incalci M (1994) Cyclosporin A markedly changes the distribution of doxorubicin in mice and rats. *J Pharmacol Exp Ther* **269:**22–27.

Cordon-Cardo C, O'Brien JP, Casals D, Rittman-Grauer L, Biedler JL, Melamed MR and Bertino JR (1989) Multidrug-resistance gene (P-glycoprotein) is expressed by endothelial cells at blood-brain barrier sites. *Proc Natl Acad Sci USA* **86:**695–698.

Derossi D, Calvet S, Trembleau A, Brunissen A, Chassaing G and Prochiantz A (1996) Cell internalization of the third helix of the Antennapedia homeodomain is receptor-independent. *J Biol Chem* **271:**18188–18193.

Derossi D, Chassaing G and Prochiantz A (1998) Trojan peptides: The penetratin system for intracellular delivery. *Trends Cell Biol* **8:**84–87.

Derossi D, Joliot AH, Chassaing G and Prochiantz A (1994) The third helix of the Antennapedia homeodomain translocates through biological membranes. *J Biol Chem* **269:**10444–10450.

Drion N, Lemaire M, Lefauconnier JM and Scherrmann JM (1996) Role of P-glycoprotein in the blood-brain transport of colchicine and vinblastine. *J Neurochem* **67:**1688–1693.

Ford JM and Hait WN (1990) Pharmacology of drugs that alter multidrug resistance in cancer. *Pharmacol Rev* **42:**155–199.

Gottesman MM and Pastan I (1993) Biochemistry of multidrug resistance mediated by the multidrug transporter. *Annu Rev Biochem* **62:**385–427.

Harwig SS, Swiderek KM, Lee TD and Lehrer RI (1995) Determination of disulphide bridges in PG-2, an antimicrobial peptide from porcine leukocytes. *J Peptide Sci* **1:**207–215.

Hughes CS, Vaden SL, Manaugh CA, Price GS and Hudson LC (1998) Modulation of doxorubicin concentration by cyclosporin A in brain and testicular barrier tissues expressing P-glycoprotein in rats. *J Neurooncol* **37:**45–54.

Huwyler J, Wu D and Pardridge WM (1996) Brain drug delivery of small molecules using immunoliposomes. *Proc Natl Acad Sci USA* **93:**14164–14169.

Joliot A, Maizel A, Rosenberg D, Trembleau A, Dupas S, Volovitch M and Prochiantz A (1998) Identification of a signal sequence necessary for the unconventional secretion of Engrailed homeoprotein. *Curr Biol* **8:**856–863.

Joliot A, Trembleau A, Raposo G, Calvet S, Volovitch M and Prochiantz A (1997) Association of Engrailed homeoproteins with vesicles presenting caveolae-like properties. *Development* **124:**1865–1875.

Jolliet-Riant P and Tillement JP (1999) Drug transfer across the blood-brain barrier and improvement of brain delivery. *Fundam Clin Pharmacol* **13:**16–26.

Juliano RL and Ling V (1976) A surface glycoprotein modulating drug permeability in Chinese hamster ovary cell mutants. *Biochim Biophys Acta* **455:**152–162.

Klopman G, Shi LM and Ramu A (1997) Quantitative structure-activity relationship of multidrug resistance reversal agents. *Mol Pharmacol* **52:**323–334.

Krishna R, De Jong G and Mayer LD (1997) Pulse exposure of SDZ PSC 833 to multidrug resistant P388/ADR and MCF7/ADR cells in the absence of anticancer drugs can fully restore sensitivity to doxorubicin. *Anticancer Res* **17:**3329–3334.

Kroll RA and Neuwelt EA (1998) Outwitting the blood-brain barrier for therapeutic purposes: Osmotic opening and other means. *Neurosurgery* **42:**1083–1099.

Lefrak EA, Pitha J, Rosenheim S and Gottlieb JA (1973) A clinicopathologic analysis of adriamycin cardiotoxicity. *Cancer* **32:**302–314.

Malhotra BK, Lemaire M and Sawchuk J (1994) Investigation of the distribution of eab 515 to cortical ECF and CSF in freely moving rats utilizing microdialysis. *Pharmacol Res* **11:**1223–1232.

Mangoni ME, Aumelas A, Charnet P, Roumestand C, Chiche L, Despaux E, Grassy G, Calas B and Chavanieu A (1996) Change in membrane permeability induced by protegrin 1: Implication of disulphide bridges for pore formation. *FEBS Lett* **383:**93–98.

Mankhetkorn S, Dubru F, Hesschenbrouck J, Fiallo M and Garnier-Suillerot A (1996) Relation among the resistance factor, kinetics of uptake, and kinetics of the P-glycoprotein-mediated efflux of doxorubicin, daunorubicin, 8-(*S*)-fluoroidarubicin, and idarubicin in multidrug-resistant K562 cells. *Mol Pharmacol* **49:**532–539.

Mayer LD (1998) Future developments in the selectivity of anticancer agents: Drug delivery and molecular target strategies. *Cancer Metastasis Rev* **17:**211–218.

Ohnishi T, Tamai I, Sakanaka K, Sakata A, Yamashima T, Yamashita J and Tsuji A (1995) In vivo and in vitro evidence for ATP-dependency of P-glycoprotein-mediated efflux of doxorubicin at the blood-brain barrier. *Biochem Pharmacol* **49:**1541–1544.

Pardridge WM (1997) Drug delivery to the brain. *J Cereb Blood Flow Metab* **17:**713–731.

Pardridge WM and Landaw EM (1984) Tracer kinetic model of blood-brain barrier transport of plasma protein- bound ligands. Empiric testing of the free hormone hypothesis. *J Clin Invest* **74:**745–752.

Rousselle CH, Lefauconnier JM and Allen DD (1998) Evaluation of anesthetic effects on parameters for the in situ rat brain perfusion technique. *Neurosci Lett* **257:**139–142.

Schroeder U, Sommerfeld P, Ulrich S and Sabel BA (1998) Nanoparticle technology for delivery of drugs across the blood-brain barrier. *J Pharmacol Sci* **87:**1305–1307.

Schwarze SR, Ho A, Vocero-Akbani A and Dowdy SF (1999) In vivo protein transduction: Delivery of a biologically active protein into mouse. *Science (Wash DC)* **285:**1569–1572.

Smith QR (1996) Brain perfusion systems for studies of drug uptake and metabolism in the central nervous system. *Pharm Biotechnol* **8:**285–307.

Takasato Y, Rapoport SI and Smith QR (1984) An in situ brain perfusion technique to study cerebrovascular transport in the rat. *Am J Physiol* **247:**H484–H493.

Triguero D, Buciak J and Pardridge WM (1990) Capillary depletion method for quantification of blood-brain barrier transport of circulating peptides and plasma proteins. *J Neurochem* **54:**1882–1888.

Tsuji A (1998) P-glycoprotein-mediated efflux transport of anticancer drugs at the blood-brain barrier. *Ther Drug Monit* **20:**588–590.

Van Asperen J, Van Tellingen O, Tijssen F, Schinkel AH and Beijnen JH (1999) Increased accumulation of doxorubicin and doxorubicinol in cardiac tissue of mice lacking mdr1a P-glycoprotein. *Br J Cancer* **79:**108–113.

Send reprint requests to: Dr. Jamal Temsamani, Synt:em, Parc Scientifique Georges Besse, 30000 Nîmes, France. E-mail: jtemsamani@syntem.eerie.fr